

1 **Single-cell transcriptomic reveals temporal dynamics of critical regulators of germ**
2 **cell fate during mouse sex determination**

3 **Authors:** Chloé Mayère^{1,2}, Yasmine Neirijnck¹, Pauline Sararols¹, Isabelle Stévant^{1,2},
4 Françoise Kühne¹, Anne Amandine Chassot³, Marie-Christine Chaboissier³, Emmanouil
5 T. Dermitzakis^{1,2}, Serge Nef^{1,2,*}.

6 **Affiliations:**

7 ¹Department of Genetic Medicine and Development, University of Geneva, 1211 Geneva,
8 Switzerland;

9 ²iGE3, Institute of Genetics and Genomics of Geneva, University of Geneva, 1211
10 Geneva, Switzerland;

11 ³Université Côte d'Azur, CNRS, Inserm, iBV, France;

12 **Lead Contact:**

13 *Corresponding Author: Serge.Nef@unige.ch

14 **Summary**

15 **Despite the importance of germ cell differentiation for sexual reproduction, gene**
16 **networks underlying their fate remain unclear. Here, we describe a comprehensive**
17 **characterization of gene expression dynamics during sex determination based on**
18 **single-cell RNA sequencing on 14,750 XX and XY mouse germ cells between**
19 **embryonic days 10.5 and 16.5. By computational gene regulation inference analysis,**
20 **we identified sex-specific, sequential waves of master regulator genes during germ**
21 **cells differentiation and unveiled that the meiotic initiator *Stra8* is regulated by**
22 **positive and negative master regulators acting in an antagonistic fashion. Consistent**
23 **with the importance of the somatic environment, we found that rare adrenal germ**
24 **cells exhibit delayed meiosis and display altered expression of master genes**
25 **controlling the female and male genetic programs. Our study provides a molecular**
26 **roadmap of germ cell sex determination at single-cell resolution that will serve as a**
27 **valuable resource for future studies of gonad development, function and disease.**

28 **Keywords:**

29 Single-cell RNA-Sequencing (scRNA-seq), sex determination, ovary, testis, gonocytes,
30 oocytes, prospermatogonia, meiosis, gene regulatory network, regulon

31 **Introduction**

32 In mice, primordial germ cells (PGCs) arise in the posterior proximal epiblast around
33 embryonic day (E) 6.25. PGCs rapidly proliferate and colonize the gonads at around
34 E10.5 (Saitou and Yamaji, 2012; Tam and Snow, 1981). The germ cell fate depends on
35 sex-specific somatic cues provided by the ovarian and testicular environments rather than
36 the chromosomal sex of the germ cells themselves (Byskov and Saxen, 1976; Evans et
37 al., 1977; McLaren, 1983).

38 In fetal ovaries, germ cells enter meiosis asynchronously in a wave from anterior to
39 posterior over about 2 days, between E12.5 and E14.5 (Bullejos and Koopman, 2004;
40 Menke et al., 2003; Yao et al., 2003). This entry into meiosis is considered a hallmark of
41 commitment to oogenesis. It is triggered by the expression of the pre-meiotic marker
42 *Stra8* and the meiosis-associated gene *Rec8* and, at the same time, by the downregulation
43 of pluripotency markers such as *Oct4 (Pou5f1)*, *Sox2* and *Nanog* (Baltus et al., 2006;
44 Bowles et al., 2006; Bullejos and Koopman, 2004; Koubova et al., 2014; Koubova et al.,
45 2006; Menke et al., 2003; Yao et al., 2003).

46 In contrast, germ cells in fetal testes differentiate into prospermatogonia through a
47 number of distinct, potentially interrelated events that occur asynchronously over a period
48 of several days, but this does not involve entry into meiosis (for a review see (Kocer et
49 al., 2009) and (Spiller and Bowles, 2019)). Germ cells adopting the male fate up-regulate
50 cell-cycle inhibitors such as *Cdkn2b* (Western et al., 2008) and are mitotically arrested
51 from E12.5 onward (McLaren, 1984). They transiently activate the NODAL/CRIPTO
52 signaling pathway (Souquet et al., 2012; Spiller et al., 2012a; Spiller et al., 2012b) and
53 down-regulate pluripotency genes such as *Nanog*, *Sox2* and *Pou5f1* (Western et al.,

54 2010). From E13.5 onward, they begin to express male-specific genes including Nanos
55 homolog 2 (*Nanos2*) (Suzuki and Saga, 2008), *Dnmt3l* (La Salle et al., 2004) and *Piwil4*
56 (Aravin et al., 2008) , which ensure normal male gametogenesis by regulating
57 spermatogonial stem cell properties.

58 Although the cellular origins of oogonia and spermatogonia are well documented,
59 numerous open questions related to the molecular mechanisms underlying their
60 differentiation and cell fate remain. For instance, the transcriptional programs mediating
61 germ cell sex determination are incompletely understood, and the essential genes and
62 transcriptional regulators orchestrating such specifications remain poorly defined. In
63 developing ovaries, the factors regulating *Stra8* expression are still questioned, and in
64 developing testes it is unclear how the different events mediating the commitment and
65 differentiation of germ cells toward spermatogenesis are initiated and coordinated.
66 Finally, our understanding of how the somatic environment, whether gonadal or extra-
67 gonadal, directs the transcriptional cascade mediating entry into meiosis and the
68 commitment to oogenesis is still unclear.

69 To date, most transcriptional analyses relevant for mouse or human germ cell sex
70 determination have been conducted using traditional methods such as microarrays or bulk
71 RNA-seq on either whole gonads or isolated germ cell populations at few selected time
72 points (Gkountela et al., 2015; Guo et al., 2015; Houmard et al., 2009; Irie et al., 2015;
73 Jameson et al., 2012; Lesch et al., 2013; Molyneaux et al., 2004; Rolland et al., 2008;
74 Rolland et al., 2011; Small et al., 2005; Soh et al., 2015; Tang et al., 2015). These studies,
75 although informative, provided only an average transcriptional summary, masking the
76 inherent variability of individual cells and lineage types and thereby limiting their

77 capacity to reveal the precise dynamics of gene expression during germ cell sex
78 determination.

79 To determine the sequence of transcriptional events that is associated with germ cell
80 commitment and differentiation toward oogenesis and spermatogenesis, we performed
81 time-series single-cell RNA sequencing (scRNA-seq) on developing gonads. We
82 recovered 14,750 germ cells from XX and XY gonads across five developmental time
83 points from E10.5 to E16.5, encompassing the entire developmental process of gonadal
84 sex determination and differentiation. We reconstructed the developmental trajectories of
85 male and female germ cells, characterized the associated genetic programs, and predicted
86 gene regulatory networks that regulate germ cell commitment and differentiation. In
87 particular, we found (i) sex-specific, sequential waves of master regulator genes during
88 germ cells differentiation, (ii) the meiotic initiator *Stra8* is regulated by positive and
89 negative master regulators acting in an antagonistic fashion, (iii) mRNA transcription and
90 mRNA splicing are often disconnected, either temporally or in a sex-specific manner, and
91 (iv) ectopic XY adrenal germ cells enter into meiosis with delay together with significant
92 alterations in ovarian-specific genes and upregulation of testis-specific genes.

93 **Results**

94 **A single-cell transcriptional atlas of germ cells sex determination and differentiation**

95 To generate a gene expression atlas of germ cells sex determination, we used droplet-
96 based 3' end scRNA-seq (10x Genomics Chromium) of XX and XY gonads from mouse
97 embryos at five developmental stages (E10.5, E11.5, E12.5, E13.5, and E16.5) (**Fig. 1A**

98 **and B**). The selected time points cover the entire process of gonadal sex determination
99 and span the emergence and differentiation of the major testicular and ovarian lineages
100 including the gonocytes. For each of the 10 conditions, we generated two independent
101 replicates from different pregnancies and sequenced an average of 10,000 cells. The
102 transcriptomes of the individual cells were sequenced at the depth of ~150,000 reads/cell.
103 Using ten well-established germ cell markers, namely *Ddx4*, *Dazl*, *Mael*, *Dppa3*, *Sycp3*,
104 *Pecam*, *Pou5f1*, *Stra8*, *Dmrt1*, and *Dnmt1*, we identified 14,750 germ cells among a total
105 of 92,267 cells (**Fig. S1A-C**) (see also **Supplementary information**). Among germ cells,
106 8,248 were XX (55.9%) and 6,502 were XY (44.1%). It included 70 cells from E10.5,
107 953 cells from E11.5, 4,365 cells from E12.5, 6,593 cells from E13.5 and 2,769 cells
108 from E16.5. As expected, the median count of UMIs and median number of detected
109 genes were higher in germ cells than in somatic cells with 22,584 versus 14,650 and
110 5,536 and 4,502, respectively (**Fig. S1D**) (Soumillon et al., 2013).

111 **Cell lineage reconstruction identifies the dynamics of gene expression during XX** 112 **and XY germ cell sex determination**

113 UMAP projection of the 14,750 germ cells (**STAR Methods**) revealed that at early stages
114 (E10.5 and E11.5), the transcriptomes of XX and XY cells globally overlapped, while
115 cells from later stages formed two sex-specific branches (**Fig. 1C and D**). We then
116 analyzed how the transcriptomes of XX and XY cells progress during the process of sex
117 determination. To order cells along a pseudotime, we used ordinal regression modeling
118 (Telley et al., 2018; Teo et al., 2010) using prior knowledge about the developmental
119 stage of each cell capture (see **Fig. 1E**, **Fig. S1E**, **STAR Methods** and **Supplementary**

120 **information**). We then represented the smoothed expression of the 3,013 top weighted
121 genes (**Table S1**) in two distinct ordinal regression models trained on XY and XX cells
122 with a double heatmap in which the center represents the earliest cells (pseudotime 0,
123 E10.5 cells) and the extremities represent the lineage endpoints (pseudotime 100, E16.5)
124 of XX germ cells (left) and XY germ cells (right), respectively (see **Supplementary**
125 **information**). The heatmap revealed that XX and XY germ cells diverged as early as
126 E12.5, exhibiting dynamic and sex-specific differentiation programs mediated by
127 thousands of genes (**Fig. S2**). In addition, using 67 well-known genes involved in mouse
128 germ cell pluripotency, sexual development and differentiation (Hill et al., 2018; Spiller
129 and Bowles, 2019), we confirmed that our single-cell data accurately recapitulated male
130 and female germ cell specification and was consistent with available literature (**Fig. 1F**).

131 **Reconstructing Gene Regulatory Networks mediating germ cell sex determination**

132 The identity and transcriptional state of a cell emerges from an underlying gene
133 regulatory network (GRN or regulome) in which the activities of a small number of key
134 transcription factors and co-factors regulate each other and their downstream target genes
135 (Aibar et al., 2017). To comprehensively infer the GRNs at play during XX and XY germ
136 cell sex determination, we applied the pySCENIC pipeline (Aibar et al., 2017) to our
137 single-cell data. In brief, SCENIC links cis-regulatory sequence information together with
138 scRNA-seq data. It first catalogs coexpression modules between transcription factors and
139 candidate target genes and then identifies modules for which the regulator's binding
140 motif is significantly enriched across target genes; it then creates regulons with only
141 direct target genes. Finally, the activity of each regulon is attributed to each cell, using

142 the AUCell method (Aibar et al., 2017). For germ cells, we identified 837 regulons (512
143 positive and 325 negative regulons) containing 13,381 genes (**Table S2**). These genes
144 represented 62% of the total number of genes (21,553) detected in germ cells, indicating
145 that our GRN analysis was comprehensive, covering the majority of the germ cell
146 transcriptome. The size of each regulon varied from 2 to 2,625 genes, with a median size
147 of 19 genes. To compare how XX and XY germ cells acquire their sex-specific identity,
148 we selected the 394 positive regulons with AUCell-determined activity in more than
149 1,000 cells (activity score >0) and classified them according to their expression pattern
150 into 30 profiles or modules (M1 to M30) along pseudotime (**Fig. 2**). We represented the
151 smoothed regulon expression level of XX and XY germ cells with a double heatmap, in
152 which the center represents the starting point of the lineage (pseudotime 0, E10.5) and the
153 extremities represent the lineage endpoints (pseudotime 100, E16.5) of the XX germ cells
154 (left) and the XY germ cells (right), respectively (**Fig. 2**). Strikingly, the expression
155 patterns revealed numerous transient, sex-specific regulon profiles, mostly at late
156 developmental stages (late E13.5 and E16.5). Initially, two modules common to both XX
157 and XY gonocytes (M20 and M17) were observed at early developmental stages, which
158 were superseded sequentially by a handful of transient and overlapping sex-specific
159 regulon modules (M10, M16 and M29 in XX germ cells, and M12, M5 and M14 in XY
160 germ cells). By late E13.5 and E16.5, we noted numerous oogonia-specific (M1, M30,
161 M21, M28, M6, and M18) and spermatogonia-specific modules (M11, M24, M9, M22,
162 M4, M3, M2 and M23).

163 We also selected 303 negative regulons with AUCell-determined activity in more than
164 1000 cells (activity score >0) and classified them according to their expression pattern

165 into 10 modules (M1 to M10) (**Fig. S3**). Negative regulons all displayed activity in
166 opposition to their repressing master regulator (data not shown) and most of them showed
167 a pattern with high expression at early times points, and a progressive
168 downregulation/repression over time (M6, M1, M7 and M2 containing 264 regulons).
169 Among them, regulons of M1 and M7 could be distinguished by the onset of their sex-
170 specific repression: regulons from modules 1 and 7 started to be repressed at E16.5 and
171 E13.5 in XY germ cells, respectively, while in XX germ cells this repression was
172 observed at E13.5 and E16.5, respectively. We also detected 4 modules formed by 34
173 regulons with sequential transient expression (M3, M4, M8 and M10). Among these,
174 target genes belonging to regulons of module 3 were transiently repressed specifically in
175 XY germ cells, in accordance with the male-specific expression of their 12 master
176 regulators (data not shown).
177 Overall, we identified 697 regulons whose activities were grouped under 40 modules
178 based on their sex-specific and temporal expression. The transient, sequential, and often
179 sex-specific profiles likely represent a sequential/hierarchical organization of regulatory
180 modules required for oogonia and spermatogonia differentiation.

181 **Sex-specific, sequential waves of cell cycle gene expression during germ cells** 182 **differentiation**

183 Following PGC colonization of the gonad around E10.5, XX and XY gonocytes undergo
184 rapid mitotic proliferation while maintaining pluripotency (McLaren, 2003; Surani et al.,
185 2007). How germ cells exit the rapid proliferative phase and enter into mitotic arrest in
186 testes, or meiosis in ovaries, remains poorly understood. Our scRNA-seq analysis

187 allowed us to comprehensively evaluate the expression of multiple key genes involved in
188 the pluripotency and proliferation of germ cells during their sex-specific differentiation.
189 We observed dynamic regulation and a strong sexual dimorphism among mitotic genes
190 between XX and XY germ cells (**Fig. 3** and **Fig. S4**). As expected, we observed in both
191 XX and XY gonocytes around E11.5 a downregulation of transcription factors mediating
192 pluripotency such as *Nanog*, *Pou5f1* (*Oct4*) as well as other pluripotency-associated
193 genes, including *Dppa2* and *Dppa4* (Maldonado-Saldivia et al., 2007; Pesce and Scholer,
194 2001; Surani et al., 2007; Western et al., 2005). The profile was similar for genes
195 regulating G1-S phase, including the genes encoding Cyclin A2, B1, D3 (*Ccna2*, *Ccnb1*,
196 *Ccnd3*) as well as E2F transcription factor genes *E2f1*, *E2f2*, *E2f3*, *E2f7*, and *E2f8*. In XY
197 germ cells, consistent with mitotic arrest in G0 between E12.5 and E14.5, we observed an
198 upregulation of cell-cycle inhibitors essential in the control of G1/G0 arrest, including
199 *Cdkn1b* (*p27^{Kip1}*) and *Cdkn2b* (*p15^{INK4b}*) around E13.5, followed by *Cdkn1c* (*p57^{Kip2}*),
200 *Cdkn2a* (*p16^{INK4a}*) and *Cdkn2c* (*p18^{INK4c}*) at E16.5. These results confirmed and extended
201 previous studies (Western et al., 2008).

202 In XX germ cells, we observed sequential waves of sex-specific upregulation of cell-
203 cycle genes including genes encoding Cyclin H, B2 and G1 (*Ccnh*, *Ccnb2*, *Ccng1*) and
204 the cell cycle inhibitor *Cdkn1a* (*p21^{Cip1}*) around E12.5, cyclins C, E1, E2, D1 (*Ccnc*,
205 *Ccne1*, *Ccnde2*, *Ccnd1*), E2F transcription factor genes *E2f1*, *E2f2*, and the cell cycle
206 inhibitor genes *Cdkn2a* (*p16^{INK4a}*), *Cdkn2c* (*p18^{INK4c}*), *Cdkn2d* (*p19^{INK4d}*) around E13.5, as
207 well as genes encoding Cyclins B3, C, O, J (*Ccnb3*, *Ccnc*, *Ccno*, *Ccnj*), and E2F
208 transcription factor genes *E2f4*, *E2f5* at E16.5. Overall, our scRNA-seq analysis

209 accurately revealed the complex and sex-specific expression of cell cycle regulators when
210 germ cells exit the proliferative phase and either arrest mitotically or enter meiosis.

211 **Predicting regulatory factors promoting meiosis and *Stra8* expression**

212 Numerous studies have attempted to identify factors regulating the expression of *Stra8*
213 (Stimulated by Retinoic Acid 8 gene), which triggers the DNA duplication step that
214 precedes meiosis, thus engaging the meiotic program in germ cells (Baltus et al., 2006).
215 Retinoic acid (RA) has been proposed as a meiosis initiating substance (Bowles et al.,
216 2006; Koubova et al., 2006) as it induces *Stra8* mRNA accumulation in RA-treated P19
217 pluripotent cell lines (Oulad-Abdelghani et al., 1996), but recent lines of evidence
218 indicated that RA signaling is actually dispensable for entry into meiosis, but instead
219 stabilizes *Stra8* expression (Kumar et al., 2011; Vernet et al., 2019). To acquire a better
220 understanding of the signals instructing oogonia to transition from mitosis to meiosis, we
221 took advantage of our GRN analysis and investigated the positive and negative regulons
222 predicted to control the expression of *Stra8* and *Rec8*, a gene that encodes a component
223 of the cohesin complex accumulating during the meiotic S-phase. Consistent with the
224 literature, *Stra8* and *Rec8* were transiently upregulated in XX germ cells between E12.5
225 and E16.5, coinciding with the entry into meiosis (**Fig. 2B** and **4B**). GRN analysis
226 revealed that both *Stra8* and *Rec8* expressions were predicted to be regulated by a
227 combination of positive and negative master regulators (**Fig. 4A, B** and **Fig. S5**). In
228 particular, *Stra8* was predicted to be negatively regulated by the mitotic cohesin RAD21
229 and the Y-box binding protein YBX1. Both factors were downregulated specifically in
230 developing XX germ cells, while expression was maintained in XY germ cells (**Fig. 4B**).

231 In parallel, the histone demethylase KDM5A (Jumonji/JARID1) and the transcription
232 factor PBX3, both preferentially expressed in XX over XY germ cells (**Fig. 4B**), were
233 predicted to be key positive regulators of *Stra8* (Ge et al., 2018). KDM5A is also a positive
234 regulator of *Ythdc2*, a gene encoding an RNA helicase that acts as critical regulator of the
235 transition from mitosis to meiosis in both male and female germlines (Bailey et al., 2017;
236 Gonczy et al., 1997). *Rec8* expression was predicted to also be negatively regulated by
237 RAD21 and YBX1, but positively regulated, among others, by KDM5A and MSX1 and
238 MSX2, two nuclear receptors known to promote meiosis initiation by maintaining or
239 enhancing *Stra8* expression (Le Bouffant et al., 2011). EZH2, a member of the polycomb
240 repressive complex 2 (PRC2) (Margueron and Reinberg, 2011), also appeared as a
241 positive regulator of *Rec8* expression that could act in concert with KDM5A to allow
242 control of chromatin opening and the correct timing of the mitosis-to-meiosis transition.
243 Overall, applying single-cell regulatory network inference to germ cell sex determination
244 leads to the prediction of new critical regulators of meiosis as well as *Stra8* and *Rec8*
245 expression.

246 **Variable rates of mRNA splicing in male and female germ cells**

247 mRNA splicing represents another powerful mechanism to modulate gene expression and
248 is known to contribute to the fine-tuning of cell differentiation programs (Kalsotra and
249 Cooper, 2011). To investigate splicing dynamics, we applied RNA velocity analysis to
250 the developing mouse germ cells to estimate the rates of nascent (unspliced) and mature
251 (spliced) transcripts during germ cell differentiation and evaluated whether there were
252 gene- or sex-specific differences in transcriptome kinetics. Velocity analysis considers

253 both spliced and unspliced mRNA counts to predict developmental trajectories and speed
254 of cell state transitions (La Manno et al., 2018). Consistent with our previous analyses,
255 we observed strong directional flow toward the most differentiated germ cells, both in the
256 XX and XY branches (**Fig. S6**). We then ordered the cells according to our ordinal
257 regression model and examined the temporal progression of RNA biogenesis of XX and
258 XY germ cells during the process of sex determination. As expected, unspliced mRNAs
259 consistently preceded spliced mRNAs (**Fig. 5**). We also observed variation in
260 transcriptomic kinetics. For example, among the meiotic-related genes, *Rec8* and *Stra8*
261 exhibited fast kinetics with little differences between unspliced and spliced mRNAs
262 whereas genes such as *Hormad2*, *Msh5*, *Tex11*, and *Spo11* exhibited increasing delays in
263 spliced transcripts (**Fig. 5A**).

264 We also investigated the rates of mature and immature transcripts of some of the genes
265 previously described as regulators of *Stra8* and *Rec8* expression (**Fig. 5B**) or as being
266 involved in mitosis (**Fig. 5C**). In several cases, we observed a significant disconnection
267 between transcription (i.e. the presence of unspliced mRNA) and the presence of mature
268 (spliced) mRNAs. For example, this was the case for the aforementioned RNA helicase
269 gene *Ythdc2*. *Ythdc2* exhibited increasing levels of unspliced transcripts in both XX and
270 XY cells (dotted lines in **Fig. 5B**, top panel) along pseudotime, but spliced mRNAs were
271 present only in XX germ cells (solid lines in **Fig. 5B**, top panel), suggesting male-specific
272 intronic retention or degradation of *Ythdc2* mRNAs. The Cyclin gene *Ccnb3* also
273 revealed sex-specific differences in gene splicing (**Fig. 5C**, fourth panel). While a
274 transient sequential increase of unspliced and spliced mRNAs was observed in XX germ
275 cells around E16.5, only unspliced mRNAs were observed in XY germ cells at late

276 E16.5. A similar pattern was observed for Cyclin *Ccnd3* (**Fig. 5C**, bottom panel). Overall,
277 we observed gene-specific or sex-specific putative intronic retention in numerous genes,
278 emphasizing once more the importance of post-transcriptional regulation in male and
279 female germ cell lineages.

280 **Ectopic adrenal germ cells also enters into meiosis, but numerous major**
281 **transcriptional regulators of oocyte differentiation are absent or downregulated**

282 While the majority of PGCs migrate toward the gonadal ridges, a small fraction of germ
283 cells are lost along the way and end up in extragonadal organs such as the nearby adrenal
284 glands and mesonephroi (Heeren et al., 2016; Upadhyay and Zamboni, 1982; Zamboni
285 and Upadhyay, 1983). These adrenal germ cells, irrespective of their genetic sex, have
286 been reported to undergo meiosis, differentiate into oocytes and display morphological
287 characteristics identical to those of young oocytes in primordial follicles before
288 disappearing around 3 weeks of age (Upadhyay and Zamboni, 1982; Zamboni and
289 Upadhyay, 1983). To evaluate how an extragonadal somatic environment affects germ
290 cell fate, we investigated at the transcriptional level how ectopic adrenal germ cells enter
291 into meiosis and commit toward the female fate.

292 Time-series 3' single-cell RNA sequencing of developing mouse adrenal cells from
293 E12.5, E13.5, E16.5, and E18.5 XY embryos identified 312 adrenal germ cells based on
294 the expression of the classical germ cell markers *Dazl*, *Ddx4* and *Mael* (see **STAR**
295 **methods**). Overall, we captured 187 adrenal germ cells at E12.5, 92 cells at E13.5, 18
296 cells at E16.5, and 15 cells at E18.5. The relatively low number of germ cells at later
297 stages may reflect the smaller proportion of germ cells in the growing adrenal glands.

298 UMAP representation of these 312 XY adrenal germ cells combined with 14,718 gonadal
299 germ cells revealed that the transcriptome of XY adrenal germ cells partially overlapped
300 with the transcriptome of XX ovarian germ cells, suggesting that their transcriptomes are
301 similar and that XY adrenal germ cells enter into meiosis and differentiate into oocytes in
302 synchrony with gonadal oocytes (**Fig. 6A**). However, a more refined analysis
303 investigating the expression of selected key marker genes mediating germ cell
304 specification revealed a more complex picture. First, meiosis-related genes, including
305 *Stra8*, *Sycp1*, *Sync3*, *Spo11*, *Ccdc155*, *Dmc1*, *Mei1*, *Mei4*, *Meioc*, *Hormad1*, *Hormad2*,
306 *Msh5*, *Tex11*, *Prdm9* and *Smc1b* displayed similar profiles and expression levels between
307 XY adrenal germ cells and XX ovarian germ cells (**Fig. 6B** and **Fig. S7**). Only a slight
308 temporal delay was observed in adrenal germ cells. One notable exception was *Rec8*,
309 whose expression was blunted in adrenal compared to ovarian germ cells (**Fig. S7**). These
310 results confirmed published data that meiosis is not significantly affected in ectopic
311 adrenal germ cells (Upadhyay and Zamboni, 1982; Zamboni and Upadhyay, 1983).
312 While several genes and master regulators of oogonia differentiation were unaffected
313 (e.g. cyclins *Ccnb3*, *Ccne2*; *Pparg*; the histone demethylases *Kdm5a* and *Phf8*; *Brca2*)
314 (**Fig. S7**), we found numerous key female genes exhibiting either downregulation or a
315 testis-like profile. It included, for example, genes involved in the WNT- β -catenin
316 pathway (*Axin2*, *Lef1*, and *Sp5*), the transcription factor genes *Msx1* and *Msx2*, the cell
317 cycle gene *E2f1*, and the oocyte-specific basic helix-loop-helix transcription factor gene
318 *Figla* (**Fig. 6B** and **Fig. S7**). Finally, we found that most genes and master regulators
319 involved in male germ cell fate were not upregulated in adrenal germ cells with few
320 notable exceptions including the male fate marker *Nanos2*, the NODAL target genes

321 *Lefty1* and *Lefty2*, the retinoic receptor gene *Rara*, the male germ cell regulator gene
322 *Ctcf1* and the spermatogonial stem cell self-renewal gene *Lhx1* (**Fig. 6B** and **Fig. S7**).
323 Overall, these results indicated that ectopic adrenal germ cells enter into meiosis at
324 around the same time as ovarian germ cells, but numerous genes and master regulators
325 related to both the female and male genetic programs were misregulated.

326 **Discussion**

327 This study represents the first large-scale scRNA-seq analysis of germ cells throughout
328 the gonadal sex determination and differentiation process. The large number of individual
329 germ cells profiled, both XX and XY, allowed us to reconstruct a continuous
330 representation of changes in gene expression occurring during the process of gonadal
331 differentiation, including the mitosis-to-meiosis switch in germ cells in developing
332 ovaries, and spermatogonial commitment and differentiation in fetal testes. This
333 represents a major advance beyond previous work and has broad implications for studies
334 in germ cell development, sex determination and the etiology of human germ cell
335 diseases.

336 How do germ cells commit to and acquire sex-specific fates during differentiation of the
337 gonad into a testis or an ovary? Our experimental design based on scRNA sequencing to
338 profile five developmental stages encompassing gonadal sex differentiation is well suited
339 to tracing gene regulatory programs in which specific combinations of transcription
340 factors drive sex- and cell type-specific transcriptomes in germ cells. Through
341 computational analyses, we have comprehensively constructed the GRNs for XX and XY

342 germ cells during the process of sex differentiation. We found that the gene regulatory
343 circuitry mediating germ cell sex determination is composed of 512 positive regulons that
344 can be grouped into 30 modules, each of them exhibiting transient, sequential and often
345 sex-specific profiles. The fact that regulons are grouped into modules that display
346 transient sex-specific profiles suggests a sequential organization of regulatory modules
347 that work together to fine-tune the interrelated cellular events that lead to XX and XY
348 germ cell differentiation. The master regulator genes present in each specific module may
349 not be controlling a single cellular event, but instead a combination of overlapping sex-
350 specific developmental processes including mitotic arrest, suppression of pluripotency
351 genes, prospermatogonia commitment and *de novo* methylation for XY germ cells, as
352 well as entry into meiosis, and suppression of pluripotency genes for XX germ cells.

353 This regulome analysis also provides an opportunity to identify new critical master
354 regulators of germ cell sex determination. While various master regulators have already
355 been implicated in playing a key role in pluripotency and germ cell sex-specific
356 commitment and differentiation, such as *Dazl*, *Pou5f1*, *Dmc1*, *Rec8*, *Stra8*, *Nodal*,
357 *Nanos2*, and *Dnmt3l*, our analysis predicted more than 800 positive and negative regulons
358 (**Fig. 2**, **Fig. S3** and **Table S2**), including a large set of new potentially critical regulators
359 of germ cell commitment and differentiation, for example KDM5A, KDM5B, NR3C1
360 and PHF8. While most of these remain predictions, they provide an important framework
361 and guide for future experimental investigation.

362 Identifying the molecules controlling the fundamental decision of germ cells to exit the
363 cell cycle and enter meiosis represents a major challenge for the reproductive medicine
364 community. An example of the usefulness of such a regulome is provided by the

365 prediction of new factors positively and negatively regulating *Stra8* expression. STRA8
366 is the only gatekeeper described to date that engages the meiotic program in developing
367 female germ cells (Baltus et al., 2006). The onset of *Stra8* expression in germ cells of the
368 developing ovary and its lack of expression in germ cells of the developing testis led to a
369 search for the presence of the female “meiosis-initiating substance” (MIS) or male
370 “meiosis-preventing substance” (MPS) (Kocer et al., 2009; McLaren and Southee, 1997).
371 While RA has emerged as a potential MIS (Bowles et al., 2006; Koubova et al., 2006),
372 recent reports revealed that female germ cells enter meiosis normally even in the absence
373 of RA signaling (Kumar et al., 2011; Vernet et al., 2019) . Our regulome analysis
374 revealed that the expression of both *Stra8* and *Rec8* is regulated by a combination of
375 positive and negative master regulators. Among them, two factors, RAD21 and YBX1,
376 are predicted to act as negative regulators of both *Stra8* and *Rec8* expression. *Rad21* and
377 *Ybx1* genes are initially expressed in both developing ovary and testis but are specifically
378 downregulated in developing ovaries at the time of entry into meiosis. Among the
379 positive regulators, we found the transcription factor PBX3 and KDM5A, a histone
380 demethylase, transiently expressed in XX germ cells around E13.5 when *Stra8* is
381 upregulated. KDM5A has recently been shown to regulate temperature-dependent sex
382 determination in red-eared slider turtle by promoting the transcription of the male sex-
383 determining gene *Dmrt1* (Ge et al., 2018). Interestingly, KDM5A also acts as a negative
384 regulator for the expression of *Rad21* and *Ybx1*, suggesting mutual antagonism between
385 the male RAD21/YBX1 factors and KDM5A/PBX3 female factors in regulating *Stra8*
386 expression and the entry into meiosis.

387 Another relevant master regulator is the nuclear receptor MSX2, a member of the Msh
388 homeobox gene family composed of three members (*Msx1*, 2 and 3). MSX1 and MSX2
389 function cooperatively to control the regulation of primordial germ cell migration (Sun et
390 al., 2016) and later in XX germ cells to promote meiosis initiation by maintaining or
391 enhancing *Stra8* expression (Le Bouffant et al., 2011). We found that *Msx2* regulon
392 activity as well as *Msx1* and *Msx2* gene expression are present in module 16, consistent
393 with their dual function (**Fig. 2** and **Fig. 4B**). *Msx2* is expressed in both XX and XY
394 PGCs by E10.5 and E11.5 and then is rapidly downregulated in XY germ cells. In
395 contrast, *Msx1* is specifically upregulated in XX germ cells from E11.5 onward with a
396 peak around E13.5 (**Fig. 4B**). We found 66 predicted target genes regulated positively by
397 the master regulator MSX2. Among these genes, we found for example *Msx1*, *Rec8*,
398 *Dlx3*, *Lef1*, *Sp5*, *Axin2*, *E2f1*, *Notch1* (**Table S2**).

399 As alluded above, two histone demethylases KDM5A (also called Jarid1A, RBP2) and
400 KDM5B (also called Jmjd3, Jarid1B or RBP2-H1) have been identified as master
401 regulators specifically expressed in E13.5 XX germ cells (**Fig. 2** and **Fig. 4B**). KDM5A
402 and KDM5B are histone demethylases that specifically demethylate H3K4me2/me3 and
403 H3K27me3, respectively. Both histone demethylases are involved in epigenetic
404 regulation of transcription and are essential for embryonic development (Christensen et
405 al., 2007; Dahl et al., 2016; Klose et al., 2007). We found that both *Kdm5a* and *Kdm5b*
406 genes are transiently expressed in XX germ cells around E13.5 in modules 13 and 14,
407 respectively (**Fig. 2** and **Fig. 4B**). In male rat, KDM5A has been shown to be also
408 expressed in quiescent gonocytes, mitotic gonocytes and spermatogonia at 6 dpp, and in
409 spermatocytes at 12, 15 and 18 dpp (Nishio et al., 2014). We identified more than 2625

410 and 1116 predicted positive target genes for KDM5A and KDM5B in germ cells
411 including *Ctnnb1* (beta catenin 1), DEAD-Box Helicases *Ddx4* and *Ddx6*, the Retinoic
412 Acid Receptor alpha (*Rara*) and the Lysine Demethylase *Kdm2a*, *Kdm2b* and *Kdm3a*, the
413 RNA binding protein *Dazl* and the Mitogen-Activated Protein Kinase Kinase Kinase 4
414 *Map3k4* (Table S2). The biological functions of KDM5A and KDM5B, particularly in
415 the context of XX germ cell meiosis regulation and oocyte differentiation remains poorly
416 characterized.

417 **Splicing kinetics and intron retention as post-transcriptional regulation in** 418 **developing germ cells**

419 Cellular RNAs are regulated at multiple stages, including transcription, RNA maturation,
420 and degradation. To study posttranscriptional regulation, and more precisely RNA
421 processing, during the process of germ cell sex determination we evaluated the
422 abundance of nascent (unspliced) and mature (spliced) mRNAs in the 14,750 XX and XY
423 germ cells. We exploited the fact that 23% of reads contained unspliced intronic
424 sequences when performing single-cell RNA-seq based on the 10x Genomics Chromium
425 protocols (La Manno et al., 2018). Although these splicing events are usually located at
426 the very 3' end of mRNA transcripts due to the oligo-dT-based protocol, the RNA
427 velocity analysis approach can be used to directly estimate unspliced and spliced mRNAs
428 present in single cells (La Manno et al., 2018).

429 We found a large variation in splicing kinetics. When analyzing, for example, meiosis-
430 related genes we identified genes with rapid splicing (e.g. *Stra8*, *Rec8*) as well as genes
431 with variable delays in splicing (e.g. *Hormad2*, *Sycp1*, *Spo11*, *Tex11*). This suggested that

432 splicing retention is another layer of post-transcriptional regulation in developing germ
433 cells, ensuring precise temporal expression of meiotic and differentiation genes. In
434 addition, we identified genes with sex-specific intronic retention/degradation patterns.
435 One example is the RNA helicase YTHDC2, a critical regulator of the transition from
436 mitosis to meiosis in both male and female germline (Bailey et al., 2017; Gonczy et al.,
437 1997). YTHDC2, through post-transcriptional control of RNA, both down-regulates the
438 mitotic program and facilitates the proper expression of meiotic and differentiation genes.
439 *Ythdc2* mutant male and female mice are infertile and mutant germ cells show defects
440 soon after the mitosis to meiosis transition (Bailey et al., 2017). Consistent with its role in
441 ensuring a transition from mitosis to meiosis, *Ythdc2* expression profile displayed a
442 female-specific upregulation between E13.5-E16.5. However, RNA velocity analysis
443 revealed the presence of unspliced *Ythdc2* mRNAs in both XX and XY germ cells,
444 suggesting that in XY germ cells these unspliced mRNAs remain immature or are
445 degraded in a sex-specific manner. Two other examples are provided by the Cyclins
446 *Ccnb3* and *Ccnd3*, which both displayed increasing levels of unspliced mRNAs in XY
447 germ cells without the presence of mature mRNAs. Intron retention has been shown to be
448 a prominent feature of the meiotic transcriptome of mouse spermatocytes (Naro et al.,
449 2017). It can either favor accumulation, storage, and timely usage of specific transcripts
450 during highly organized cell differentiation programs or cause transcript instability at
451 specific developmental transitions (Edwards et al., 2016; Naro et al., 2017; Pimentel et
452 al., 2016; Wong et al., 2013; Yap et al., 2012). The temporal or sex-specific variation in
453 intronic retention appears to be surprisingly frequent during the process of germ cell sex
454 determination and may ensure proper and timely expression of selected transcripts.

455 **Comparing adrenal and gonadal germ cells development provides a tool to**
456 **investigate the importance of the somatic environment in the process of oogenesis**

457 By comparing the transcriptome of adrenal and gonadal germ cells, we have been able to
458 investigate how germ cells respond to three different somatic environments: the adrenal,
459 ovarian and testicular environments. It allowed us to also investigate whether the gene
460 regulatory circuitries mediating germ cell sex determination, composed of 837 regulons,
461 are interconnected or act independently. The dynamic expression pattern of key marker
462 genes of meiosis is strikingly similar in both adrenal and ovarian germ cells with a slight
463 delay in adrenal germ cells. It suggests that the initiation and maintenance of meiosis
464 proceeds relatively normally in adrenal germ cells. However, we also observed a
465 significant alteration in the expression of some key female master regulator genes as well
466 as upregulation of male master regulator genes, indicating that the somatic environment
467 in the adrenal gland cannot completely support a female fate for these gonocytes. In
468 particular, we observed a lack of upregulation of genes involved in the canonical
469 WNT/ β -catenin signaling pathway (*Axin2*, *Lef1*, and *Sp5*), suggesting that germ cells in
470 this environment are unable to respond to WNT signals, or to express their receptors.
471 This may also explain the slight delay in adrenal meiosis progression (Chassot et al.,
472 2011; Chassot et al., 2008; Naillat et al., 2010). Other master regulator genes such as the
473 transcription factor genes *Msx1* and *Msx2*, *Cdx2* and the oocyte-specific basic helix-loop-
474 helix transcription factor gene *Figla* also displayed significant alteration. Interestingly,
475 the absence of *Msx1* and *Msx2* expression may explain why *Rec8* expression, but not
476 other meiotic genes such as *Stra8*, is blunted in adrenal germ cells (**Fig. S7**). Based on

477 our GRN analysis, we found that both MSX1 and MSX2 are strong positive regulators of
478 *Rec8* expression (**Fig. 4A**). Concerning male-specific master regulators, the large
479 majority of them are not expressed in XY adrenal germ cells but with few notable
480 exceptions including *Nanos2*, *Lefty1*, *Lefty2*, *Rara*, *Ctcf1*, *Lhx1*. Overall, the adrenal
481 environment does not provide all the necessary signal(s) required to commit germ cells to
482 oogenesis, resulting in adrenal germ cells characterized by an altered identity and delayed
483 meiosis.

484 Compiling single cell transcriptomes from mouse germ cells at five developmental stages
485 during the process of sex determination, both in gonadal and extragonadal tissues,
486 allowed us to provide a comprehensive insight into the sex-specific genetic programs and
487 gene regulatory networks that regulate germ cell commitment toward a male or female
488 fate. As such, we have created a valuable and rich resource for the broad biology
489 community that should provide insights into how this fundamental decision impacts the
490 etiology of infertility and human gonadal germ cell tumours, two of the main clinical
491 consequences of defects in germ cell sex determination.

492 **Acknowledgments:**

493 This work was supported by grants from the Swiss National Science Foundation (grants
494 31003A_173070 and 51PHI0-141994) and by the Département de l'Instruction Publique
495 of the State of Geneva (to S.N.). We thank Luciana Romano and Deborah Penet for the
496 sequencing, Cécile Gameiro and Gregory Schneiter (Flow Cytometry Facility, University
497 of Geneva), the team of the Animal Facility (Faculty of Medicine, University of Geneva),

498 Julien Prados (Basic Neuroscience, University of Geneva) for his help for pseudotime
499 computation and Valentin Durand Graphic Design for help with artwork. We thank also
500 Andy Greenfield, the members of the Nef and Dermitzakis laboratories for helpful
501 discussion and critical reading of the manuscript.

502 **Author Contributions**

503 Conceptualization, S.N.; data generation and investigation, C.M., Y.N., P.S., A.A.C., I.S.
504 and F.K.; Formal Analysis and Data Curation, C.M and P.S.; Writing – Original Draft,
505 S.N., C.M., and M.-C.C.; Funding Acquisition, S.N., and E.T.D.; Resources, S.N., and
506 E.T.D.; Supervision, S.N., and E.T.D.

507 **Declaration of Interests**

508 The authors declare no competing interests

509 **STAR Methods:**

510 **KEY RESOURCES TABLE**

REAGENT or RESOURCE	SOURCE	IDENTIFIER
Chemicals, Peptides, and Recombinant Proteins		
Trypsin-EDTA (0.05%), phenol red	Thermo Fisher Scientific	25300054
DPBS, no calcium, no magnesium	Thermo Fisher Scientific	14190144
Fetal bovine serum	Thermo Fisher Scientific	26140087
Draq7™ #B25595	Beckman Coulter	B25595
Critical Commercial Assays		
Papain dissociation system	Worthington	LK003150
Chromium™ i7 Multiplex Kit	10x Genomics	120262
Chromium™ Single Cell 3' Library & Gel Bead Kit v2	10x Genomics	120237
Chromium™ Single Cell A Chip Kit	10x Genomics	1000009
Qubit dsDNA High Sensitivity	Life Technologies	Q32854
Agilent High Sensitivity DNA Kit Reagents	Agilent	5067-4626
Deposited Data		
Raw data, normalized counts	GEO	GSE136220
Scripts for analysis	GitHub	Available soon
Experimental Models: Organisms/Strains		
Mus musculus: CD-1	Charles River	Strain code 022
Mus musculus: CD-1-Tg(<i>Nr5a1</i> GFP)	(Stallings, 2002)	N/A
Oligonucleotides		
Primers for sex genotyping	(McFarlane et al., 2013)	N/A
Software and Algorithms		
Cell Ranger (version 2.3)	10X	www.10xgenomics.com
Python (version 3.6)	Python	Pyth
R (version version 3.6.1)	R-Project	https://www.R-project.org/
Seurat (Version 2.3.0)	Stuart et al, 2018	
heatmaps (version 1.8.0)	Bioconductor	https://bioconductor.org/packages/release/bioc/html/heatmaps.html
pheatmap (version 1.0.12)	Bioconductor	https://github.com/raivokolde/pheatmap
Bmm (version 4.1)	(Teo et al., 2010)	
ggplot2 (version 3.2.0)	(Wickham, 2009)	https://ggplot2.tidyverse.org
scanpy (version 1.4.4)	(Wolf et al, 2018)	https://github.com/theislab/scanpy
scvelo (version 0.1.19)		https://github.com/theislab/scvelo
matplotlib (version 3.0.3)		
pyscenic (version 0.9.14)	(Aibar et al., 2017)	
bbknn (version 1.3.5)	(Park et al, 2018)	https://github.com/Teichlab/bbknn
velocyto (version 0.17.8)	(La Manno et al 2018)	http://velocyto.org/

511 **Contact for Reagent and Resource Sharing**

512 Further information and requests for resources and reagents should be directed to and will
513 be fulfilled by the Lead Contact, Serge Nef (serge.nef@unige.ch).

514 **Experimental Model Details**

515 **Transgenic Mice**

516 All animal work was conducted according to the ethical guidelines of the Direction
517 Générale de la Santé of the Canton de Genève (experimentation ID GE/57/18).
518 *Tg(Nr5a1-GFP)* mouse strain was described previously (Stallings et al., 2002) and has
519 been maintained on a CD1 genetic background.

520 **Method Details**

521 **Mouse urogenital ridges, testes, ovaries and adrenal glands collection**

522 CD-1 female mice were bred with heterozygous *Tg(Nr5a1-GFP)* transgenic male mice.
523 Adult females were time-mated and checked for the presence of vaginal plugs the next
524 morning (E0.5). E10.5 (8±2 tail somites (ts)), E11.5 (19±4 ts), E12.5, E13.5, E16.5 and
525 E18.5 embryos were collected and the presence of the *Nr5a1-GFP* transgene was
526 assessed under UV light. Sexing of E10.5 and E11.5 embryos was performed by PCR
527 with a modified protocol from (McFarlane et al., 2013). Urogenital ridges from each sex,
528 XY adrenal glands, testes or ovaries were pooled for tissue dissociation.

529 **Single cell suspension and library preparations**

530 Urogenital ridges and adrenal glands were enzymatically dissociated at 37°C for 20 and
531 40 minutes, respectively, using the Papain dissociation system (Worthington
532 #LK003150). Cells were resuspended in DMEM 2%FBS, filtered through a 70 µm cell
533 strainer and stained with the dead cell marker Draq7™ (Beckman Coulter, #B25595).
534 Viable single cells were collected on a BD FACS Aria II by excluding debris (side scatter
535 vs. forward scatter), dead cells (side scatter vs. Draq7 staining), and doublets (height vs.
536 width). Testes and ovaries (from E12.5 to E16.5) were enzymatically dissociated at 37°C
537 during 15 minutes in Trypsin-EDTA 0.05% (Gibco #25300054), resuspended in DMEM
538 2%FBS and filtered through a 70 µm cell strainer. After counting, 3000 to 7000 single
539 cells were loaded on a 10x Chromium instrument (10x Genomics). Single-cell RNA-Seq
540 libraries were prepared using the Chromium Single Cell 3' v2 Reagent Kit (10x
541 Genomics) according to manufacturer's protocol. Each condition (organ, sex and
542 developmental stage) was performed in two biological independent replicates.

543 **Sequencing**

544 Library quantification was performed using the Qubit fluorometric assay with dsDNA HS
545 Assay Kit (Invitrogen). Library quality assessment was performed using a Bioanalyzer
546 Agilent 2100 with a High Sensitivity DNA chip (Agilent Genomics). Libraries were
547 diluted, pooled and sequenced on an Illumina HiSeq4000 using paired-end 26 + 98 bp as
548 the sequencing mode. Libraries were sequenced at a targeted depth of 100 000 to 150 000
549 total reads per cell. Sequencing was performed at the Health 2030 Genome Center,
550 Geneva.

551 **Bioinformatic Analysis**

552 **Data processing with the Cell Ranger package, cell selection and in-house quality**
553 **controls**

554 Computations were performed at the Vital-IT Center for high-performance computing of
555 the SIB (Swiss Institute of Bioinformatics) (<http://www.vital-it.ch>). Demultiplexing,
556 alignment, barcode filtering and UMI counting were performed with the Cell Ranger v2.1
557 pipeline (10x Genomics). Algorithms and versions used are listed in the key resources
558 table. Data were mapped to the mouse reference genome GRCm38.p5 in which the eGFP
559 (NC_011521.1) combined with the bovine GH 3'-splice/polyadenylation signals
560 (Stallings et al., 2002) (NM_180996.1) sequences have been added.

561 Cell-associated barcode selection and quality checks were performed with in-house tools.
562 (see **Supplementary information** for details)

563 **Gene expression normalization**

564 UMI counts per gene and per cell were divided by the total UMI detected in the cell,
565 multiplied by a scale factor of 10,000 and log transformed.

566

567 **Germ cells selection**

568 After barcode filtering based on the unique molecular identifiers (UMI) distribution, we
569 obtained 92,267 cells. It included 14,904 cells from E10.5, 16,581 cells from E11.5,
570 19,551 cells from E12.5, 25,012 cells from E13.5, and 16,219 cells from E16.5. Among
571 the 52,463 XY cells and the 39,804 XX cells, the median number of UMIs was 17,493
572 and 17,655 and the median number of detected genes was 4,802 and 4,658, respectively.

573 To determine which one were germ cells, we selected all genes detected in more than 50
574 cells, and performed ICA on log normalized values. To assess for batch effect, we built a
575 nearest neighbor graph using BBKNN function (BBKNN package). Clustering was
576 performed using Scanpy Louvain method with resolution 1 and UMAP were generated
577 using Scanpy UMAP method with default parameters. We selected clusters with a strong
578 expression of 10 well-known germ cells markers (see **Supplementary table S3** and
579 **Supplementary information** for details).

580 **Pseudotime ordering of the cells**

581 To order the cells along a pseudotime, we took advantage of the discrete prior knowledge
582 we have about the embryonic day at which each cell were harvested and generated an
583 ordinal regression model (adapted from (Teo et al., 2010)) to obtain a continuous
584 pseudotime score reflecting the differentiation status of the cells (see **Supplementary**
585 **information** for details).

586 **Gene regulatory network generation**

587 GRN analysis was generated using pyScenic package (see **Supplementary information**
588 for details).

589 **Regulons hierarchical clustering**

590 Regulons were clustered using ward.d hierarchical clustering on the AUC matrix with
591 Spearman correlation distance. Modulons were determined using cutree with k=10 for
592 negative regulons and k=30 for positive regulons.

593 **Heatmaps and expression curves**

594 Heatmaps were generated using R (packages pheatmap and heatmaps). Expression curves
595 were generated using ggplot2 (see **Supplementary information** for details).

596 **Network visualization**

597 Network views and layouts were generated with Cytoscape V3.7.1.

598 **Velocity analysis**

599 To generate spliced and unspliced counts data, the velocity.py script from velocity
600 package was called on each bam file with aforementioned reference genome annotation
601 (see **Supplementary information** for details).

602 **Ectopic adrenal germ cells analysis**

603 The analysis was performed using aforementioned steps: log normalization, ICA,
604 neighbor graph, and clustering with the same parameters. Germ cell clusters were
605 selected with the same 10 germ cell marker genes (see **Supplementary information** for
606 details). For pseudotime ordering of the cells, a model was trained on gonadal cells only
607 and the pseudotime for adrenal germ cells was predicted from it.

608 **Data and source code availability**

609 Germ cells single-cell RNA-seq data is available on GEO (accession number
610 GSE136220). Both adrenal and gonadal gene expression data are included in
611 ReproGenomics Viewer (Darde et al., 2019; Darde et al., 2015).

612 **References**

- 613 Aibar, S., Gonzalez-Blas, C.B., Moerman, T., Huynh-Thu, V.A., Imrichova, H., Hulselmans, G.,
614 Rambow, F., Marine, J.C., Geurts, P., Aerts, J., *et al.* (2017). SCENIC: single-cell regulatory
615 network inference and clustering. *Nat Methods* *14*, 1083-1086.
- 616 Aravin, A.A., Sachidanandam, R., Bourc'his, D., Schaefer, C., Pezic, D., Toth, K.F., Bestor, T.,
617 and Hannon, G.J. (2008). A piRNA pathway primed by individual transposons is linked to de
618 novo DNA methylation in mice. *Mol Cell* *31*, 785-799.
- 619 Bailey, A.S., Batista, P.J., Gold, R.S., Chen, Y.G., de Rooij, D.G., Chang, H.Y., and Fuller, M.T.
620 (2017). The conserved RNA helicase YTHDC2 regulates the transition from proliferation to
621 differentiation in the germline. *Elife* *6*.
- 622 Baltus, A.E., Menke, D.B., Hu, Y.C., Goodheart, M.L., Carpenter, A.E., de Rooij, D.G., and
623 Page, D.C. (2006). In germ cells of mouse embryonic ovaries, the decision to enter meiosis
624 precedes premeiotic DNA replication. *Nat Genet* *38*, 1430-1434.
- 625 Bowles, J., Knight, D., Smith, C., Wilhelm, D., Richman, J., Mamiya, S., Yashiro, K.,
626 Chawengsaksophak, K., Wilson, M.J., Rossant, J., *et al.* (2006). Retinoid signaling determines
627 germ cell fate in mice. *Science* *312*, 596-600.
- 628 Bullejos, M., and Koopman, P. (2004). Germ cells enter meiosis in a rostro-caudal wave during
629 development of the mouse ovary. *Mol Reprod Dev* *68*, 422-428.
- 630 Byskov, A.G., and Saxen, L. (1976). Induction of meiosis in fetal mouse testis in vitro. *Dev Biol*
631 *52*, 193-200.
- 632 Chassot, A.A., Gregoire, E.P., Lavery, R., Taketo, M.M., de Rooij, D.G., Adams, I.R., and
633 Chaboissier, M.C. (2011). RSP01/beta-catenin signaling pathway regulates oogonia
634 differentiation and entry into meiosis in the mouse fetal ovary. *PLoS One* *6*, e25641.
- 635 Chassot, A.A., Ranc, F., Gregoire, E.P., Roepers-Gajadien, H.L., Taketo, M.M., Camerino, G., de
636 Rooij, D.G., Schedl, A., and Chaboissier, M.C. (2008). Activation of beta-catenin signaling by
637 *Rspo1* controls differentiation of the mammalian ovary. *Hum Mol Genet* *17*, 1264-1277.
- 638 Christensen, J., Agger, K., Cloos, P.A., Pasini, D., Rose, S., Sennels, L., Rappsilber, J., Hansen,
639 K.H., Salcini, A.E., and Helin, K. (2007). RBP2 belongs to a family of demethylases, specific for
640 tri- and dimethylated lysine 4 on histone 3. *Cell* *128*, 1063-1076.
- 641 Dahl, J.A., Jung, I., Aanes, H., Greggains, G.D., Manaf, A., Lerdrup, M., Li, G., Kuan, S., Li, B.,
642 Lee, A.Y., *et al.* (2016). Broad histone H3K4me3 domains in mouse oocytes modulate maternal-
643 to-zygotic transition. *Nature* *537*, 548-552.
- 644 Darde, T.A., Lecluze, E., Lardenois, A., Stevant, I., Alary, N., Tuttelmann, F., Collin, O., Nef, S.,
645 Jegou, B., Rolland, A.D., *et al.* (2019). The ReproGenomics Viewer: a multi-omics and cross-
646 species resource compatible with single-cell studies for the reproductive science community.
647 *Bioinformatics*.
- 648 Darde, T.A., Sallou, O., Becker, E., Evrard, B., Monjeaud, C., Le Bras, Y., Jegou, B., Collin, O.,
649 Rolland, A.D., and Chalmel, F. (2015). The ReproGenomics Viewer: an integrative cross-species
650 toolbox for the reproductive science community. *Nucleic Acids Res* *43*, W109-116.
- 651 Edwards, C.R., Ritchie, W., Wong, J.J., Schmitz, U., Middleton, R., An, X., Mohandas, N.,
652 Rasko, J.E., and Blobel, G.A. (2016). A dynamic intron retention program in the mammalian
653 megakaryocyte and erythrocyte lineages. *Blood* *127*, e24-e34.
- 654 Evans, E.P., Ford, C.E., and Lyon, M.F. (1977). Direct evidence of the capacity of the XY germ
655 cell in the mouse to become an oocyte. *Nature* *267*, 430-431.
- 656 Ge, C., Ye, J., Weber, C., Sun, W., Zhang, H., Zhou, Y., Cai, C., Qian, G., and Capel, B. (2018).
657 The histone demethylase KDM6B regulates temperature-dependent sex determination in a turtle
658 species. *Science* *360*, 645-648.

- 659 Gkountela, S., Zhang, K.X., Shafiq, T.A., Liao, W.W., Hargan-Calvopina, J., Chen, P.Y., and
660 Clark, A.T. (2015). DNA Demethylation Dynamics in the Human Prenatal Germline. *Cell* *161*,
661 1425-1436.
- 662 Gonczy, P., Matunis, E., and DiNardo, S. (1997). bag-of-marbles and benign gonial cell neoplasm
663 act in the germline to restrict proliferation during *Drosophila* spermatogenesis. *Development* *124*,
664 4361-4371.
- 665 Guo, F., Yan, L., Guo, H., Li, L., Hu, B., Zhao, Y., Yong, J., Hu, Y., Wang, X., Wei, Y., *et al.*
666 (2015). The Transcriptome and DNA Methylome Landscapes of Human Primordial Germ Cells.
667 *Cell* *161*, 1437-1452.
- 668 Heeren, A.M., He, N., de Souza, A.F., Goercharn-Ramlal, A., van Iperen, L., Roost, M.S., Gomes
669 Fernandes, M.M., van der Westerlaken, L.A., and Chuva de Sousa Lopes, S.M. (2016). On the
670 development of extragonadal and gonadal human germ cells. *Biol Open* *5*, 185-194.
- 671 Hill, P.W.S., Leitch, H.G., Requena, C.E., Sun, Z., Amouroux, R., Roman-Trufero, M.,
672 Borkowska, M., Terragni, J., Vaisvila, R., Linnett, S., *et al.* (2018). Epigenetic reprogramming
673 enables the transition from primordial germ cell to gonocyte. *Nature* *555*, 392-396.
- 674 Houmard, B., Small, C., Yang, L., Naluai-Cecchini, T., Cheng, E., Hassold, T., and Griswold, M.
675 (2009). Global gene expression in the human fetal testis and ovary. *Biol Reprod* *81*, 438-443.
- 676 Irie, N., Weinberger, L., Tang, W.W., Kobayashi, T., Viukov, S., Manor, Y.S., Dietmann, S.,
677 Hanna, J.H., and Surani, M.A. (2015). SOX17 is a critical specifier of human primordial germ
678 cell fate. *Cell* *160*, 253-268.
- 679 Jameson, S.A., Natarajan, A., Cool, J., DeFalco, T., Maatouk, D.M., Mork, L., Munger, S.C., and
680 Capel, B. (2012). Temporal transcriptional profiling of somatic and germ cells reveals biased
681 lineage priming of sexual fate in the fetal mouse gonad. *PLoS Genet* *8*, e1002575.
- 682 Kalsotra, A., and Cooper, T.A. (2011). Functional consequences of developmentally regulated
683 alternative splicing. *Nat Rev Genet* *12*, 715-729.
- 684 Klose, R.J., Yan, Q., Tothova, Z., Yamane, K., Erdjument-Bromage, H., Tempst, P., Gilliland,
685 D.G., Zhang, Y., and Kaelin, W.G., Jr. (2007). The retinoblastoma binding protein RBP2 is an
686 H3K4 demethylase. *Cell* *128*, 889-900.
- 687 Kocer, A., Reichmann, J., Best, D., and Adams, I.R. (2009). Germ cell sex determination in
688 mammals. *Mol Hum Reprod* *15*, 205-213.
- 689 Koubova, J., Hu, Y.C., Bhattacharyya, T., Soh, Y.Q., Gill, M.E., Goodheart, M.L., Hogarth, C.A.,
690 Griswold, M.D., and Page, D.C. (2014). Retinoic acid activates two pathways required for
691 meiosis in mice. *PLoS Genet* *10*, e1004541.
- 692 Koubova, J., Menke, D.B., Zhou, Q., Capel, B., Griswold, M.D., and Page, D.C. (2006). Retinoic
693 acid regulates sex-specific timing of meiotic initiation in mice. *Proc Natl Acad Sci U S A* *103*,
694 2474-2479.
- 695 Kumar, S., Chatzi, C., Brade, T., Cunningham, T.J., Zhao, X., and Duester, G. (2011). Sex-
696 specific timing of meiotic initiation is regulated by *Cyp26b1* independent of retinoic acid
697 signalling. *Nat Commun* *2*, 151.
- 698 La Manno, G., Soldatov, R., Zeisel, A., Braun, E., Hochgerner, H., Petukhov, V., Lidschreiber,
699 K., Kastrioti, M.E., Lonnerberg, P., Furlan, A., *et al.* (2018). RNA velocity of single cells. *Nature*
700 *560*, 494-498.
- 701 La Salle, S., Mertineit, C., Taketo, T., Moens, P.B., Bestor, T.H., and Trasler, J.M. (2004).
702 Windows for sex-specific methylation marked by DNA methyltransferase expression profiles in
703 mouse germ cells. *Dev Biol* *268*, 403-415.
- 704 Le Bouffant, R., Souquet, B., Duval, N., Duquenne, C., Herve, R., Frydman, N., Robert, B.,
705 Habert, R., and Livera, G. (2011). *Msx1* and *Msx2* promote meiosis initiation. *Development* *138*,
706 5393-5402.
- 707 Lesch, B.J., Dokshin, G.A., Young, R.A., McCarrey, J.R., and Page, D.C. (2013). A set of genes
708 critical to development is epigenetically poised in mouse germ cells from fetal stages through
709 completion of meiosis. *Proc Natl Acad Sci U S A* *110*, 16061-16066.

710 Maldonado-Saldivia, J., van den Bergen, J., Krouskos, M., Gilchrist, M., Lee, C., Li, R., Sinclair,
711 A.H., Surani, M.A., and Western, P.S. (2007). Dppa2 and Dppa4 are closely linked SAP motif
712 genes restricted to pluripotent cells and the germ line. *Stem Cells* 25, 19-28.
713 Margueron, R., and Reinberg, D. (2011). The Polycomb complex PRC2 and its mark in life.
714 *Nature* 469, 343-349.
715 McFarlane, L., Truong, V., Palmer, J.S., and Wilhelm, D. (2013). Novel PCR assay for
716 determining the genetic sex of mice. *Sex Dev* 7, 207-211.
717 McLaren, A. (1983). Sex reversal in the mouse. *Differentiation* 23 *Suppl*, S93-98.
718 McLaren, A. (1984). Meiosis and differentiation of mouse germ cells. *Symp Soc Exp Biol* 38, 7-
719 23.
720 McLaren, A. (2003). Primordial germ cells in the mouse. *Dev Biol* 262, 1-15.
721 McLaren, A., and Southee, D. (1997). Entry of mouse embryonic germ cells into meiosis. *Dev*
722 *Biol* 187, 107-113.
723 Menke, D.B., Koubova, J., and Page, D.C. (2003). Sexual differentiation of germ cells in XX
724 mouse gonads occurs in an anterior-to-posterior wave. *Dev Biol* 262, 303-312.
725 Molyneaux, K.A., Wang, Y., Schaible, K., and Wylie, C. (2004). Transcriptional profiling
726 identifies genes differentially expressed during and after migration in murine primordial germ
727 cells. *Gene Expr Patterns* 4, 167-181.
728 Naillat, F., Prunskaitė-Hyyryläinen, R., Pietila, I., Sormunen, R., Jokela, T., Shan, J., and Vainio,
729 S.J. (2010). Wnt4/5a signalling coordinates cell adhesion and entry into meiosis during
730 presumptive ovarian follicle development. *Hum Mol Genet* 19, 1539-1550.
731 Naro, C., Jolly, A., Di Persio, S., Bielli, P., Setterblad, N., Alberdi, A.J., Vicini, E., Geremia, R.,
732 De la Grange, P., and Sette, C. (2017). An Orchestrated Intron Retention Program in Meiosis
733 Controls Timely Usage of Transcripts during Germ Cell Differentiation. *Dev Cell* 41, 82-93 e84.
734 Nishio, H., Hayashi, Y., Moritoki, Y., Kamisawa, H., Mizuno, K., Kojima, Y., and Kohri, K.
735 (2014). Distinctive changes in histone H3K4 modification mediated via Kdm5a expression in
736 spermatogonial stem cells of cryptorchid testes. *J Urol* 191, 1564-1572.
737 Oulad-Abdelghani, M., Bouillet, P., Decimo, D., Gansmuller, A., Heyberger, S., Dolle, P.,
738 Bronner, S., Lutz, Y., and Chambon, P. (1996). Characterization of a premeiotic germ cell-
739 specific cytoplasmic protein encoded by *Stra8*, a novel retinoic acid-responsive gene. *J Cell Biol*
740 135, 469-477.
741 Pesce, M., and Scholer, H.R. (2001). Oct-4: gatekeeper in the beginnings of mammalian
742 development. *Stem Cells* 19, 271-278.
743 Pimentel, H., Parra, M., Gee, S.L., Mohandas, N., Pachter, L., and Conboy, J.G. (2016). A
744 dynamic intron retention program enriched in RNA processing genes regulates gene expression
745 during terminal erythropoiesis. *Nucleic Acids Res* 44, 838-851.
746 Rolland, A.D., Jegou, B., and Pineau, C. (2008). Testicular development and spermatogenesis:
747 harvesting the postgenomics bounty. *Adv Exp Med Biol* 636, 16-41.
748 Rolland, A.D., Lehmann, K.P., Johnson, K.J., Gaido, K.W., and Koopman, P. (2011). Uncovering
749 gene regulatory networks during mouse fetal germ cell development. *Biol Reprod* 84, 790-800.
750 Small, C.L., Shima, J.E., Uzumcu, M., Skinner, M.K., and Griswold, M.D. (2005). Profiling gene
751 expression during the differentiation and development of the murine embryonic gonad. *Biol*
752 *Reprod* 72, 492-501.
753 Soh, Y.Q., Junker, J.P., Gill, M.E., Mueller, J.L., van Oudenaarden, A., and Page, D.C. (2015). A
754 Gene Regulatory Program for Meiotic Prophase in the Fetal Ovary. *PLoS Genet* 11, e1005531.
755 Soumillon, M., Necsulea, A., Weier, M., Brawand, D., Zhang, X., Gu, H., Barthes, P., Kokkinaki,
756 M., Nef, S., Gnirke, A., *et al.* (2013). Cellular source and mechanisms of high transcriptome
757 complexity in the mammalian testis. *Cell Rep* 3, 2179-2190.
758 Souquet, B., Tourpin, S., Messiaen, S., Moison, D., Habert, R., and Livera, G. (2012). Nodal
759 signaling regulates the entry into meiosis in fetal germ cells. *Endocrinology* 153, 2466-2473.

- 760 Spiller, C., and Bowles, J. (2019). Sexually dimorphic germ cell identity in mammals. *Curr Top*
761 *Dev Biol* 134, 253-288.
- 762 Spiller, C.M., Bowles, J., and Koopman, P. (2012a). Regulation of germ cell meiosis in the fetal
763 ovary. *Int J Dev Biol* 56, 779-787.
- 764 Spiller, C.M., Feng, C.W., Jackson, A., Gillis, A.J., Rolland, A.D., Looijenga, L.H., Koopman,
765 P., and Bowles, J. (2012b). Endogenous Nodal signaling regulates germ cell potency during
766 mammalian testis development. *Development* 139, 4123-4132.
- 767 Stallings, N.R., Hanley, N.A., Majdic, G., Zhao, L., Bakke, M., and Parker, K.L. (2002).
768 Development of a transgenic green fluorescent protein lineage marker for steroidogenic factor 1.
769 *Mol Endocrinol* 16, 2360-2370.
- 770 Sun, J., Ting, M.C., Ishii, M., and Maxson, R. (2016). Msx1 and Msx2 function together in the
771 regulation of primordial germ cell migration in the mouse. *Dev Biol* 417, 11-24.
- 772 Surani, M.A., Hayashi, K., and Hajkova, P. (2007). Genetic and epigenetic regulators of
773 pluripotency. *Cell* 128, 747-762.
- 774 Suzuki, A., and Saga, Y. (2008). Nanos2 suppresses meiosis and promotes male germ cell
775 differentiation. *Genes Dev* 22, 430-435.
- 776 Tang, W.W., Dietmann, S., Irie, N., Leitch, H.G., Floros, V.I., Bradshaw, C.R., Hackett, J.A.,
777 Chinnery, P.F., and Surani, M.A. (2015). A Unique Gene Regulatory Network Resets the Human
778 Germline Epigenome for Development. *Cell* 161, 1453-1467.
- 779 Telley, L., Agirman, G., Prados, J., Fièvre, S., Oberst, P., Vitali, I., Nguyen, L., Dayer, A., and
780 D., J. (2018). Single-cell transcriptional dynamics and origins of neuronal diversity in the
781 developing mouse neocortex. *BioRxiv*.
- 782 Teo, C.H., Vishwanthan, S.V.N., Smola, A.J., and Le, Q.V. (2010). Bundle Methods for
783 Regularized Risk Minimization. *Journal of Machine Learning Research* 11, 311–336.
- 784 Upadhyay, S., and Zamboni, L. (1982). Ectopic germ cells: natural model for the study of germ
785 cell sexual differentiation. *Proc Natl Acad Sci U S A* 79, 6584-6588.
- 786 Vernet, N., Mark, M., Condrea, D., Féret, B., Klopfenstein, M., Alunni, V., Teletin, M., and
787 Ghyselinck, N.B. (2019). Meiosis Initiates In The Fetal Ovary Of Mice Lacking All Retinoic
788 Acid Receptor Isoforms. *BioRxiv*.
- 789 Western, P., Maldonado-Saldivia, J., van den Bergen, J., Hajkova, P., Saitou, M., Barton, S., and
790 Surani, M.A. (2005). Analysis of *Esg1* expression in pluripotent cells and the germline reveals
791 similarities with *Oct4* and *Sox2* and differences between human pluripotent cell lines. *Stem Cells*
792 23, 1436-1442.
- 793 Western, P.S., Miles, D.C., van den Bergen, J.A., Burton, M., and Sinclair, A.H. (2008). Dynamic
794 regulation of mitotic arrest in fetal male germ cells. *Stem Cells* 26, 339-347.
- 795 Western, P.S., van den Bergen, J.A., Miles, D.C., and Sinclair, A.H. (2010). Male fetal germ cell
796 differentiation involves complex repression of the regulatory network controlling pluripotency.
797 *FASEB J* 24, 3026-3035.
- 798 Wong, J.J., Ritchie, W., Ebner, O.A., Selbach, M., Wong, J.W., Huang, Y., Gao, D., Pinello, N.,
799 Gonzalez, M., Baidya, K., *et al.* (2013). Orchestrated intron retention regulates normal
800 granulocyte differentiation. *Cell* 154, 583-595.
- 801 Yao, H.H., DiNapoli, L., and Capel, B. (2003). Meiotic germ cells antagonize mesonephric cell
802 migration and testis cord formation in mouse gonads. *Development* 130, 5895-5902.
- 803 Yap, K., Lim, Z.Q., Khandelia, P., Friedman, B., and Makeyev, E.V. (2012). Coordinated
804 regulation of neuronal mRNA steady-state levels through developmentally controlled intron
805 retention. *Genes Dev* 26, 1209-1223.
- 806 Zamboni, L., and Upadhyay, S. (1983). Germ cell differentiation in mouse adrenal glands. *J Exp*
807 *Zool* 228, 173-193.

808 **Figure legends**

809 **Figure 1. Generation of the germ cell sex determination atlas.** (A) Schematic
810 representation of developing testis and ovary highlighting the major events of male and
811 female germ cell differentiation as well as the time points used in the study. (B)
812 Illustration of the experimental workflow using the 10x Genomics Chromium platform.
813 UMAP Projection of 14,750 germ cells colored by time (C), sex (D) and computed
814 pseudotime going from 0 (E10.5 cells) to 100 (E16.5 cells) (E). (F) Heatmap of 67 well
815 known genes involved in germ cell differentiation. Cells were ordered using a pseudotime
816 score generated with ordinal regression modeling, expression was smoothed to reduce
817 dropout effect and obtain a better visualization of expression tendencies (expression
818 scale: log normalized counts normalized per gene). Cells with lowest score (E10.5) are in
819 the center of the figure and those with highest scores (E16.5) are on the left side for XX
820 cells and on the right side for XY cells. The relevant processes regulated by these genes
821 (cell cycle, male sex determination, meiosis, pluripotency and others) are indicated on the
822 left side of the heatmap.

823 **Figure 2. Gene regulation network analysis reveals transient patterns of**
824 **transcription activation during germ cell sex determination.** (A) Activity (see STAR
825 method) heatmap of the 394 regulons with positive association with their master
826 regulator. Regulons were clustered in 30 modules (M1-M30) using hierarchical clustering
827 with Spearman correlation distance. Cells were ordered according to their pseudotime
828 score with lowest score (E10.5) in the center of the figure and highest score (E16.5) on
829 the left side for XX cells and on the right side for XY cells. Boxes on the right display
830 examples of master regulators of interest that are colored by dominant activity in XX

831 (pink) or XY (blue) cells. In brackets is the number of target genes for each master
832 regulator. (B) Smoothed expression heatmap of well known marker genes involved in
833 germ cells differentiation. Expression scale: log normalized counts normalized per gene.

834 **Figure 3. Sex-specific, sequential waves of cell cycle genes during germ cells**
835 **differentiation.** Smoothed expression heatmap of cell cycle genes. Cells were ordered
836 according to their pseudotime. Cells with lowest score (E10.5) are in the center of the
837 figure and those with the highest scores (E16.5) are on the left side for XX cells and on
838 the right side for XY cells. Log normalized expression values were normalized per row.

839 **Figure 4. Gene regulation network of the meiotic genes *Stra8*, *Rec8* and *Ythdc2*.** (A)
840 Gene regulation network of *Rec8*, *Stra8* and *Ythdc2* with connection to their regulators.
841 Color of the edge represent positive (green) or negative (red) regulation. Edge width is
842 proportional to association score of the target gene to the master regulator. Blue and red-
843 fill colors indicate high expression in XY and XX germ cells, respectively (Log2 FC). (B)
844 Expression profiles of selected genes involved in *Rec8*, *Stra8* and *Ythdc2* gene regulation.
845 The solid line represents the smoothed expression curves of the gene in the cells ordered
846 by pseudotime, and the fade band is the 95% confidence interval of the model.

847 **Figure 5. Relative abundance of nascent (unspliced) and mature (spliced)**
848 **transcripts reveals gene- or sex-specific differences in transcriptomic kinetics.**
849 Expression profile of spliced (solid line) and unspliced (dash line) forms of transcripts in
850 XX (red) and XY (blue) germ cells across pseudotime for (A) meiosis-associated genes,
851 (B) selected regulators of *Stra8*, *Rec8* and *Ythdc2* expression and (C) mitosis-associated

852 genes. As unspliced transcripts are less detected, spliced expression levels were
853 multiplied by the gamma factor as in La Manno, 2018. In (B) UMAP projection of
854 *Ythdc2* transcripts in the cells colored by pooled abundance of spliced and unspliced
855 transcripts. Expression scale: log normalized counts.

856 **Figure 6. Altered identity and delayed meiosis in adrenal XY germ cells.** (A) UMAP
857 projections of 14,718 gonadal cells and 312 ectopic XY germ cells developing in the
858 adrenal colored by organ (left) and time (right). Adrenal germ cells are represented with
859 larger dots. (B) Expression profiles of selected genes involved in meiosis, oogenesis and
860 spermatogenesis differentiation process. The solid line represents the smoothed expression
861 curves of the gene in the cells ordered by pseudotime, and the fade band is the 95%
862 confidence interval of the model.

Figure 2

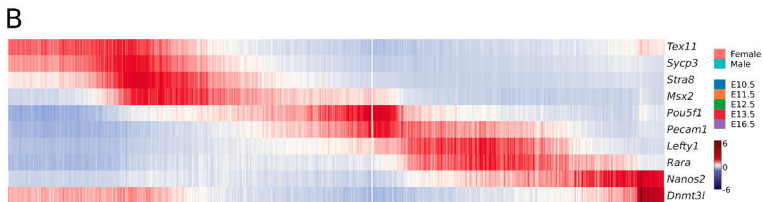
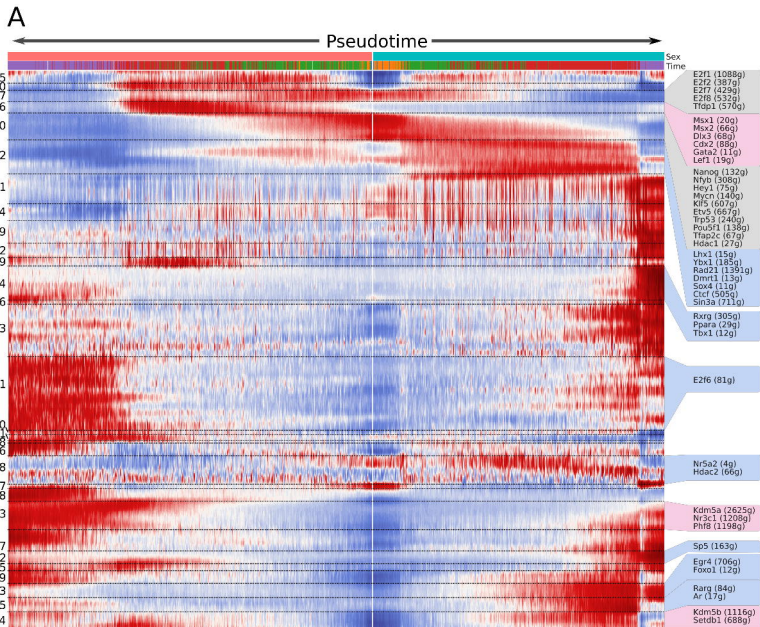


Figure 3

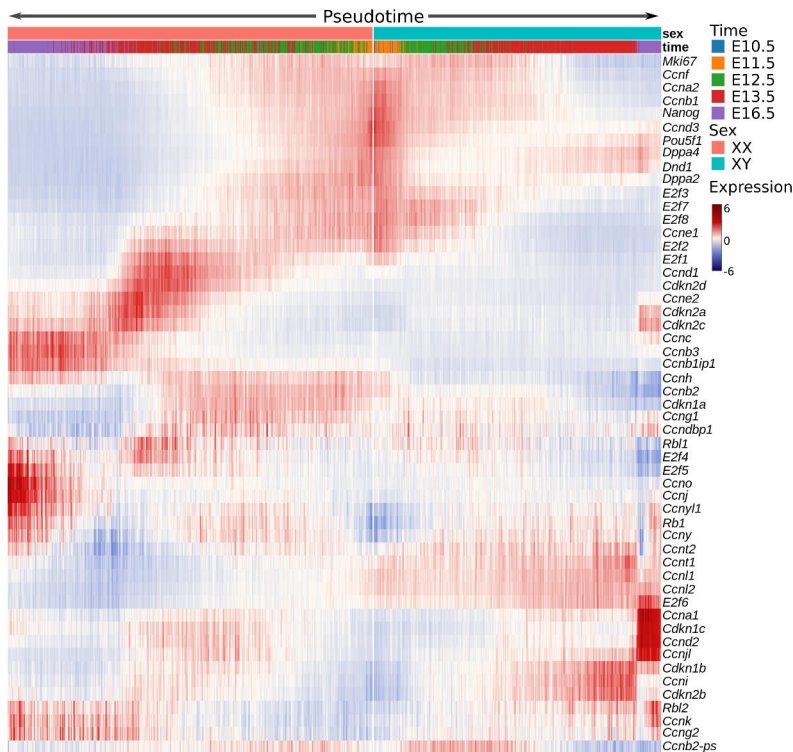
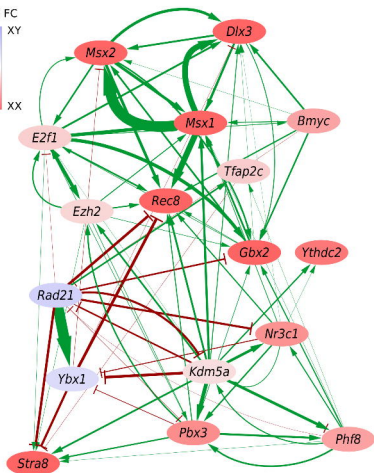
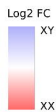


Figure 4

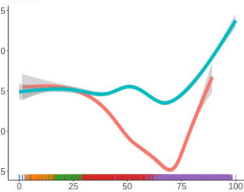
A



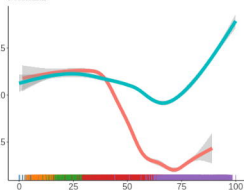
B



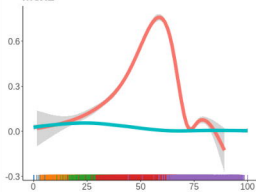
Ybx1



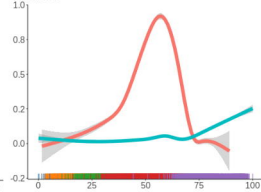
Rad21



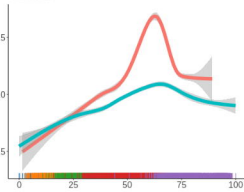
Msx1



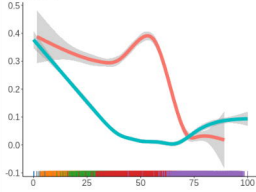
Rec8



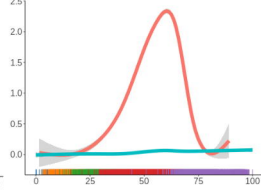
Kdm5a



Msx2



Stra8



Pbx3

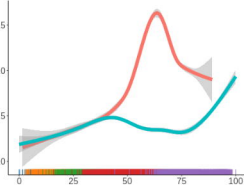


Figure 5

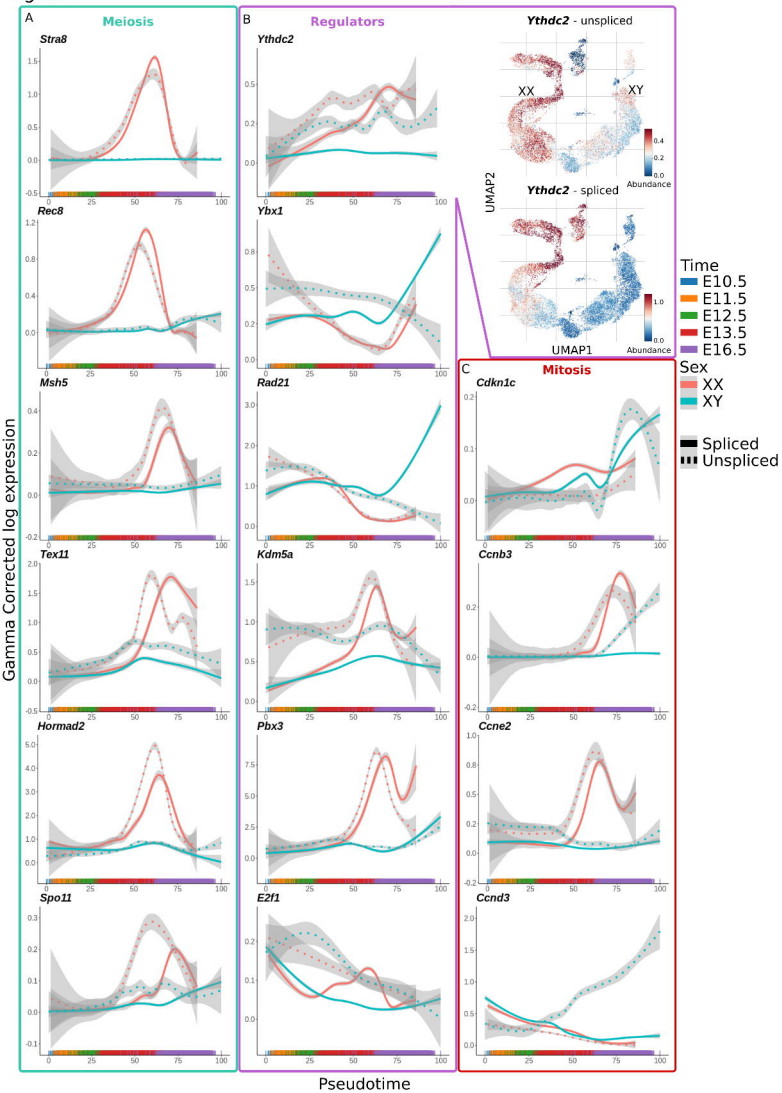


Figure 6

